DRUG DELIVERY

Boosting systemic absorption of peptides with a bioinspired buccal-stretching patch

Zhi Luo[1,2]*†, David Klein Cerrejon[2]†, Simon Römer[2], Nicole Zoratto[2], Jean-Christophe Leroux[2]*

Biopharmaceuticals, including proteins and peptides, have revolutionized the treatment of a wide range of diseases, from diabetes and cardiovascular disorders to virus infections and cancer. Despite their efficacy, most of these macromolecular drugs require parenteral administration because of their high molecular weight and relative instability. Over the past 40 years, only a few oral peptide drugs have entered clinical trials, even when formulated with substantial amounts of permeation enhancers. To overcome the epithelial barrier, devices that inject drugs directly into the gastrointestinal mucosa have been proposed recently. However, the robustness and safety of those complex systems are yet to be assessed. In this study, we introduced an innovative technology to boost drug absorption by synergistically combining noninvasive stretching of the buccal mucosa with permeation enhancers. Inspired by the unique structural features of octopus suckers, a self-applicable suction patch was engineered, enabling strong adhesion to and effective mechanical deformation of the mucosal tissue. In dogs, this suction patch achieved bioavailability up to two orders of magnitude higher than those of the commercial tablet formulation of desmopressin, a peptide drug known for its poor oral absorption. Moreover, systemic exposure comparable to that of the approved oral semaglutide tablet was achieved without further optimization. Last, a first-in-human study involving 40 healthy participants confirmed the dosage form's acceptability, thereby supporting the clinical translatability of this simple yet effective platform technology.

INTRODUCTION

Developing efficient formulation strategies to overcome biological barriers is a long-standing research interest in pharmaceutical sciences (*1*). Drug delivery systems can improve drug absorption, decrease side effects, increase patient compliance, and reduce costs for health care systems (*2*). Despite the undisputed clinical needs, success has been scarce in the oral delivery of macromolecular drugs such as peptides and proteins (*3*, *4*). After decades of research in the quest for efficient permeation-enhancing technologies, only two oral formulations of water-soluble peptides (semaglutide and octreotide) were approved by the U.S. Food and Drug Administration in the past 3 years (*5*). Unfortunately, even when large amounts of permeation enhancers (PEs) are administered and the formulation is taken under strict intake conditions, the absolute oral bioavailability of these peptides is often below 1%, and the variability remains high (*6*, *7*).

Although alternative systemic delivery approaches have been explored, including pulmonary inhalation and intranasal administration (*8*, *9*), these strategies also suffer from relatively low bioavailability and high variability. Transdermal systems, such as microneedles and iontophoretic devices, have the potential to achieve high efficiency in the systemic delivery of peptides (*10*). However, they are hindered by the complexity of manufacturing or application procedures. As a result, there has been growing interest in promoting drug absorption via receptor-mediated translocation (*11*, *12*) or more invasive physical methods (*13*), such as microneedle injection in the gastrointestinal (GI) tract (*14*–*16*). The former approach can improve the systemic delivery of peptide drugs but results in the formation of a new chemical entity, which can lengthen the development process. The latter can provide bioavailabilities comparable to those reached by subcutaneous injection; however, such a device has yet to demonstrate its robustness as well as patient acceptance (*17*). Moreover, the safety of repeated injections in the nonsterile GI tract needs further careful long-term evaluation.

Compared with other delivery sites, the buccal region has several advantages, including easy accessibility, tolerance of mechanical disruption, and avoidance of hepatic first-pass effect (*18*). In addition, the mild pH and lower proteolytic activity make the oral cavity much less hostile to peptides than the stomach and the small intestine. However, the human buccal epithelium is composed of about 40 to 50 layers of nonkeratinized cells with a thickness of 500 to 800 μm (*19*). The outermost epithelial layers are rich in intercellular lipids, derived from membrane-coating granules, that create a dense and amorphous layer filling the intercellular space and representing a key permeation barrier (*20*). Although a few buccal formulations based on mucoadhesive materials have been marketed (*21*), the typical adhesive strengths are in the order of 1 to 10 kPa (*22*) and depend largely on the hydration of the polymeric matrix (*23*). In addition, most buccal formulations reported to date are only used for the delivery of low–molecular weight (Mw) drugs (*21*). The permeation of macromolecules across the buccal mucosa has met with only limited success, even in the presence of PEs (*24*).

To increase the systemic absorption of macromolecular drugs, we developed a conceptually original noninvasive platform technology that combines mechanical stretching of the buccal mucosa with chemical PEs. We hypothesized that a mechanical disturbance might transiently loosen the mucosal cellular organization and increase intercellular spaces, leading to a higher drug permeability. To simultaneously achieve effective adhesion to and mechanical stretching of the mucosal tissue, we took inspiration from a rarely

[1]Guangdong Provincial Key Laboratory of Advanced Biomaterials, Department of Biomedical Engineering, Southern University of Science and Technology, Shenzhen, Guangdong 518055, P.R. China. [2]Institute of Pharmaceutical Sciences, Department of Chemistry and Applied Biosciences, ETH Zurich, 8093 Zurich, Switzerland.
*Corresponding author. Email: luoz@sustech.edu.cn (Z.L.); jleroux@ethz.ch (J.C.L.)
†These authors contributed equally to this work.

exploited morphological feature of octopus suckers in the design of our suction patch. Octopus suckers generally consist of two compartments (*25*), the upper domed acetabulum and the exposed disk-like infundibulum, featuring a constricted orifice in between. Mimicking such a strategic muscular arrangement could allow efficient and stable adhesion and could provide an effective means to stretch the soft tissue with a strength on the order of 100 kPa. At the same time, various types of excipients, including PEs, could be loaded inside the suction patch. The patch can also promote drug diffusion by disturbing the cellular organization and lipid barriers of the mucosa (*26*). A synergy between mechanical stretching and chemical PEs could enable a more efficient drug diffusion into the highly vascularized tissue, facilitating its access to the systemic circulation.

RESULTS

Octopus-inspired design of the suction patch

On the basis of the structural characteristics of octopus suckers (Fig. 1A), two different suction patches were designed. One is a conventional, simple suction cup (SC) (Fig. 1B), and the other is a suction cup orifice design (SCOD) (Fig. 1, C to E). The SCOD has an overall diameter of 1.1 cm and a height of 0.6 cm, comparable to commercially available mucoadhesive tablets (*21*), to minimize discomfort and allow for easy application by patients. The dome-shaped cavity inside the SCOD could be loaded with more than 50 mg of a drug, as shown with desmopressin (fig. S1). A photopolymerizable poly(β-thioether ester) polymer was synthesized (fig. S2, A and B) (*27*), and a resin was prepared for three-dimensional (3D) printing of the suction patches (*28*). The printed elastomer is nontoxic and exhibited good elasticity (Young's modulus of 1.8 ± 0.1 MPa) while being robust enough to both deform the buccal tissue and withstand multiple compression cycles without rupturing (elongation at break of 175%) (fig. S2, C and D).

Adhesion to and mechanical strain of the oral mucosa

Adhesion performance to various substrates under different conditions was assessed (fig. S3). The two patches exhibited similar adhesion strengths when applied to hard substrates like glass (52.8 ± 10.6 kPa for SC and 45.1 ± 1.0 kPa for SCOD) (fig. S3). However, when tested on a soft and deformable ShA 00 silicone substrate, the SC adhesion force decreased substantially (28.1 ± 1.4 kPa), whereas SCOD adhesion performance remained unaffected by the substrate (55.9 ± 11.2 kPa) (fig. S3). When testing the patches on porcine buccal mucosa at different pull angles, the reduction of SC adhesion performance became even more pronounced. The SC adhesion significantly ($P \leq 0.001$) decreased from 27.1 ± 1.0 kPa when pulled at 0° to 14.4 ± 3.7 kPa at 45°, whereas SCOD adhesion remained largely unaffected, exhibiting adhesion forces of 49.7 ± 6.6 kPa at 0° and 52.7 ± 6.5 kPa at 45° (fig. S3). Because of its better performance on soft tissue, SCOD patches were selected for all subsequent experiments.

To better understand the mechanical stretching of the buccal tissue caused by the SCOD, the patch was cryo-sectioned together with the tissue after 30-min applications. As shown in fig. S4 (A to C, top), the histological sections show the shape the buccal tissue adopts within the SCOD (fig. S4, A to C, top). The contour of the deformed tissue was measured (fig. S4, A to C, middle) and converted to a 3D model (fig. S4, A to C, bottom) that allowed the calculation of the effective contact surface area ($SA_{SCOD\ stretched}$). The results suggested that the suction led to a 275 ± 10% increase in the tissue surface area due to the mechanical stretching.

We then investigated the impact of mechanical strain combined with a PE on the buccal epithelium by studying the histology of freshly harvested porcine buccal mucosa after SCOD application. The patches were manually applied to the buccal mucosa for 3 hours at 37°C. Inside each SCOD, a fluorescent poorly permeable drug surrogate, sulfonated cyanine 5 (Cy5), was loaded with and without the PE sodium taurocholate (NaTaC) (*29*) and poly(vinyl alcohol) (PVA) to control drug release kinetics (fig. S5, A to C). The corresponding release profile of the formulations was measured as shown in fig. S5D. iFluor 488–conjugated phalloidin (green label for cytoskeleton, binding to F-actin) and Hoechst (blue label for cell nucleus) fluorescent staining was performed on the cryo-sectioned buccal mucosa. As shown in Fig. 2 (A to C), the basal membrane was identified by the dense alignment of blue-stained cell nuclei, which separated the mucosa (main permeation barrier) from the vascularized lamina propria and muscle tissues. In the epithelium, the unstretched and intact cell layers were characterized by the dense meshes of F-actin with a thickness of 500 to 800 μm. Inside the SCOD-deformed mucosal regions (Fig. 2A), the epithelial layer was highly stretched, featuring loosened cellular organization and thinning of the mucosa. This effect was solely dependent on the mechanical stretching and, thus, independent of the formulation used (an empty SCOD achieved a similar effect, as shown in fig. S4). The observed histological disruption was also localized and noninvasive because the outermost surface of the epithelium remained continuous after SCOD stretching.

When NaTaC was used as a PE (Fig. 2A), the F-actin signal in the mucosa largely diminished in the top part of the deformed region, especially within regions where Cy5 diffused. In contrast, when the SCOD was applied without PE (Fig. 2B), the diffusion was not promoted, nor was a reduction of the F-actin signal observed. In comparison, the NaTaC-containing SCOD was also applied without a negative pressure–induced deformation (0 kPa) (SCOD applied using an in-house–designed clamp; fig. S6). The F-actin signal reduction was observed only on the top few layers of the epithelium (Fig. 2C), which suggests that without the mechanical stretching, the PE merely acts at the mucosal surface.

Ex vivo permeation study on porcine buccal mucosa

An ex vivo study was then performed with freshly excised porcine buccal mucosa to investigate permeation. Although the model is static and neglects blood flow, it allows for the investigation of drug surrogate penetration beyond the surface epithelium layers without compromising tissue integrity and layer interfaces. After a 3-hour application of a manually applied SCOD at 37°C, the permeation profile of Cy5 was obtained by quantifying the fluorescence intensity as a function of the distance from the mucosal surface. The maximum penetration depth value (d_p) was extracted from the profile and used as an indicator for drug permeation efficiency. To identify an optimal formulation, four different PEs that are commonly used in preclinical and clinical studies were screened, including NaTaC, sodium caprate (C10), salcaprozate sodium (SNAC), and pelargonidin. Multiple fluorescent histological images were taken for each PE to calculate the d_p values (fig. S7, A to D). As shown in Fig. 3A, with the addition of C10 or NaTaC, substantially (*P* values are shown in table S1) higher d_p values (3489 ± 228 μm

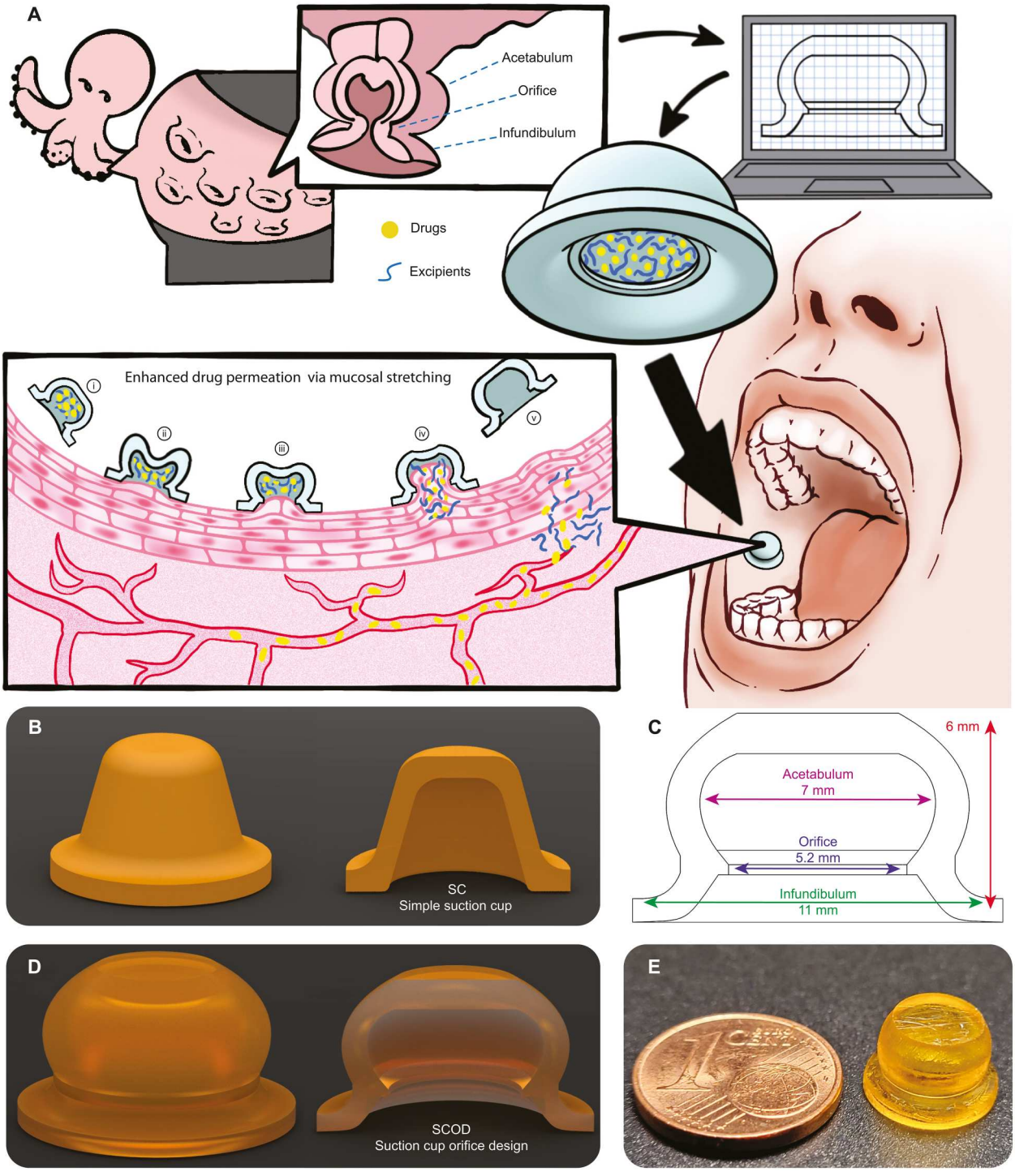

Fig. 1. A bioinspired suction patch to deliver macromolecular drugs via mechanical deformation of the oral mucosa. (**A**) Similar to octopus suckers, the SCOD features three elements: a dome-shaped acetabulum that generates hypobaric pressure and can incorporate different drug formulations, a flexible disk-like infundibulum that can adapt to various substrates, and a constricted orifice to maintain the suction patch structure and prevent leakage. The fabricated patch can then be self-applied on the buccal mucosa. The application of the dosage form includes the following steps: (i) SCOD placement; (ii) compression; (iii) mucosa deformation; (iv) drug release and permeation; and (v) removal of the SCOD. (**B**) A 3D image and a cross-sectional view of the simple suction cup (SC). (**C**) Design of the SCOD, including the dimensions of the patch elements used in the study. (**D**) A 3D image and a cross-sectional view of the SCOD. (**E**) A 3D-printed SCOD relative to a one-cent coin.

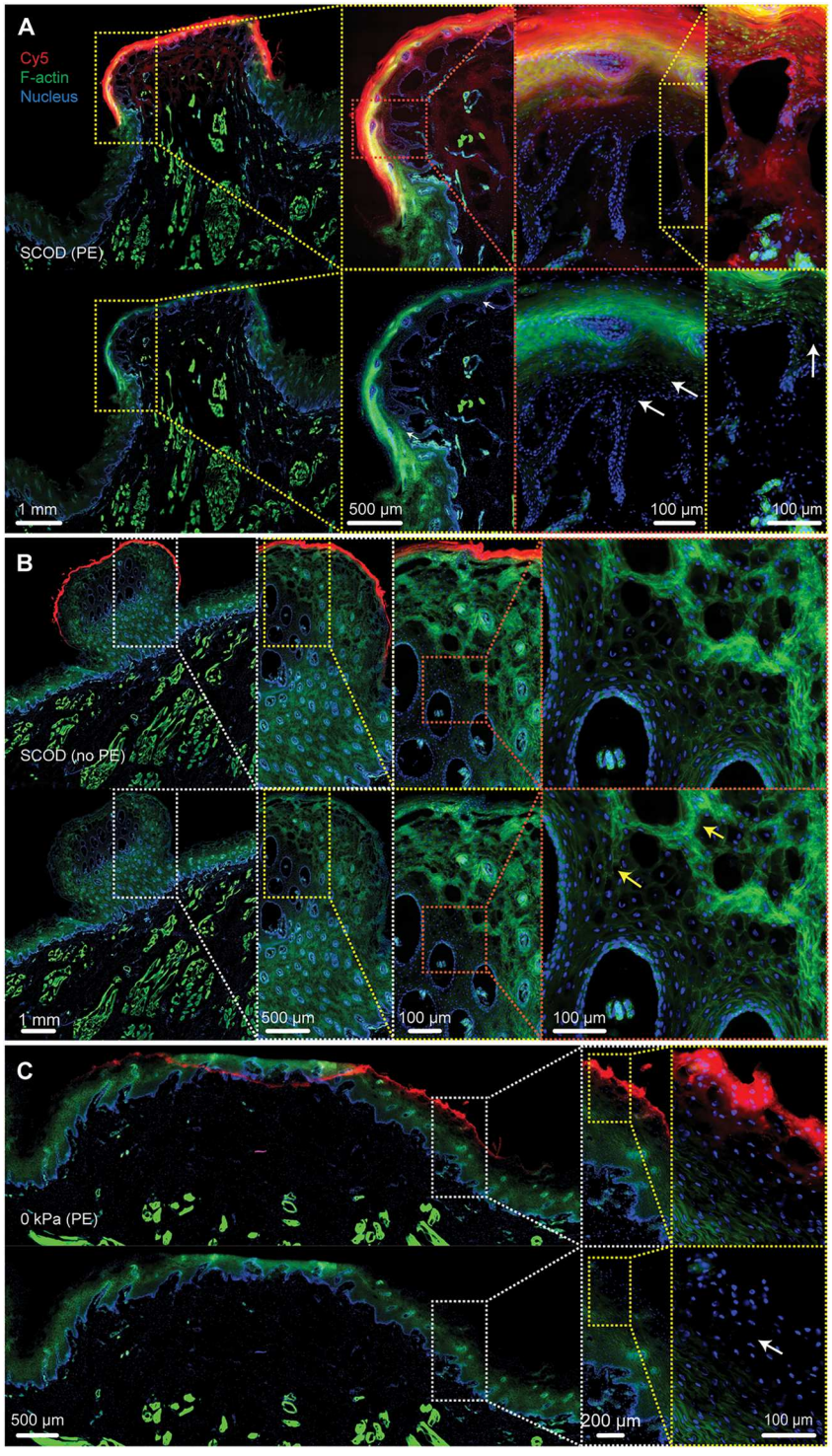

Fig. 2. Mechanistic investigation of interactions between mechanical stretching and chemical PE. (**A**) Fluorescent images of cryo-sectioned porcine buccal mucosa after a manual SCOD application at 37°C for 3 hours. SCOD was loaded with 54 μg of Cy5 (red), 1.2 mg of PVA, and 5.7 mg of NaTaC. Cytoskeleton is visualized via F-actin (green) and cell nuclei (blue) in the tissue section. The top row shows all three channels, whereas the Cy5 (red) channel was removed in the bottom row. A series of magnifications show the reduced F-actin signal (white arrows), where strong Cy5 permeation can be observed. (**B**) A similar manual SCOD application as in (A), but no NaTaC was loaded in the SCOD. A series of magnifications shows no reduction of the F-actin signal (yellow arrows) within the top section of the stretched area in the absence of NaTaC. (**C**) The SCOD [same loading as in (A)] applied without negative pressure–induced deformation (0 kPa) for 3 hours at 37°C. A series of magnifications show that the dye only penetrated the uppermost cell layers, where the reduction of the F-actin signal (white arrow) can also be observed.

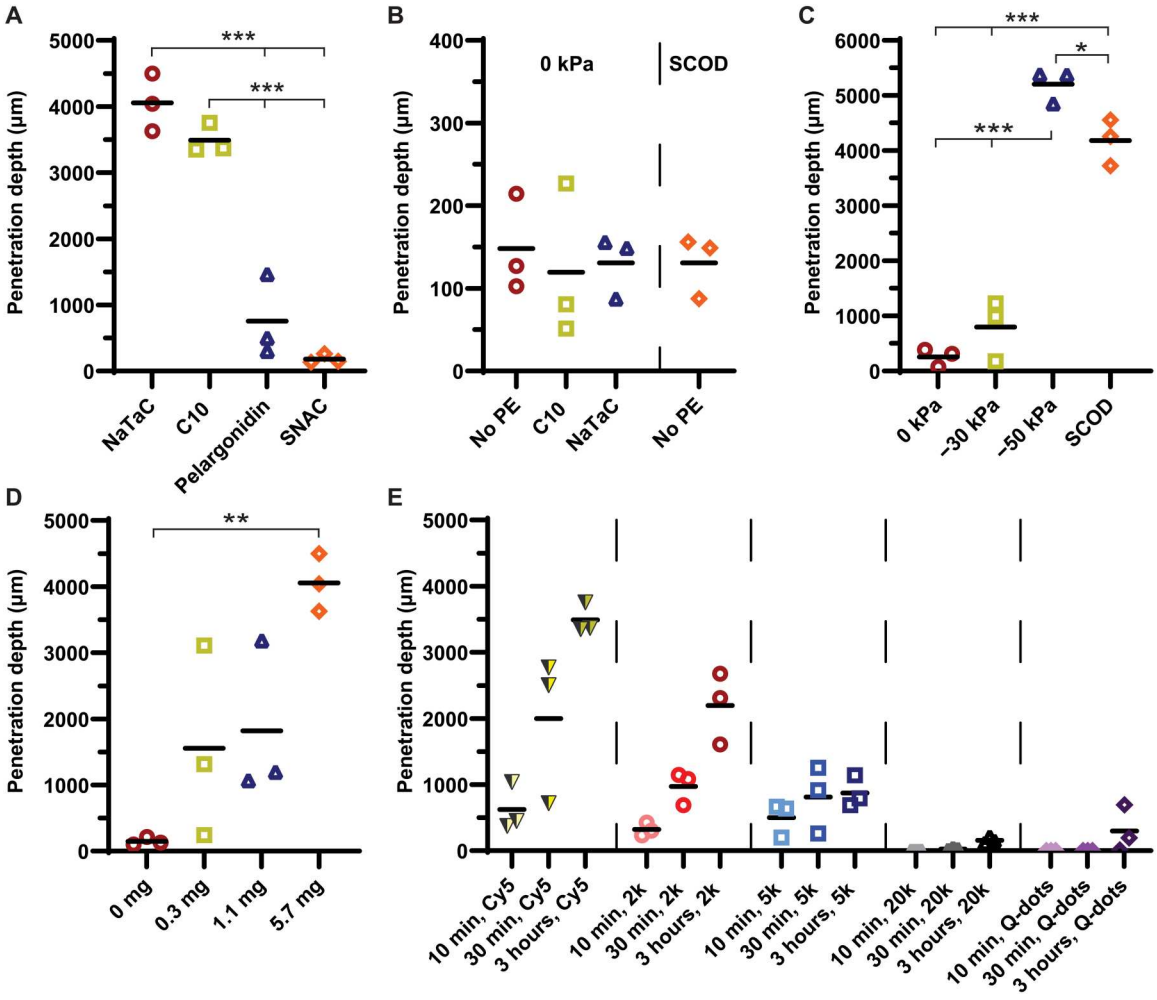

Fig. 3. Ex vivo evaluation of drug surrogate permeation. (**A**) The SCOD was loaded and manually applied for 3 hours at 37°C with 54 μg of Cy5, 1.2 mg of PVA, and different PEs (5.7 mg of NaTaC, 2.1 mg of C10, 2.9 mg of pelargonidin, or 3.2 mg of SNAC). The maximum d_p of Cy5 (50-a.u. intensity threshold) was evaluated. (**B**) Cy5 d_p analysis with the SCOD applied for 3 hours at 37°C without negative pressure (0 kPa) or manual compression (SCOD). (**C**) Cy5 d_p analysis (20-a.u. intensity threshold) with SCOD applied without negative pressure (0 kPa), a controlled negative pressure device (−30 or −50 kPa), or manual compression (SCOD). (**D**) Cy5 d_p values (50-a.u. intensity threshold) using different amounts {0 [same as in (B), 0.3, 1.1, and 5.7 mg [same as in (A)]} of NaTaC. (**E**) d_p values (50-a.u. intensity threshold) of different drug surrogates with increasing Mw {54 μg of Cy5 [same as in (A)], 0.16 mg of 2k PEG-Cy5, 0.5 mg of 5k PEG-Cy5, 0.8 mg of 20k PEG-Cy5, and 0.08 mg of Q-dots (Ø 5 nm)} with 5.7 mg of NaTaC or 2.1 mg of C10. The complete set of images and statistical analysis of d_p quantification can be found in the Supplementary Materials. Solid black lines indicate the mean d_p value (n = 3 independent experiments, 5 measurement lines each).

and 4057 ± 435 μm, respectively) were observed compared with that of SNAC (d_p = 182 ± 71 μm) and pelargonidin (d_p = 757 ± 622 μm). When a SCOD was placed onto the mucosa without inducing mechanical stretching of the tissue (0 kPa), Cy5 fluorescence was only detected on the surface of the mucosa with a d_p of 148 ± 58 μm (Fig. 3B and fig. S8A). A similar d_p value of around 150 μm was observed when the two best-performing PEs, NaTaC and C10, were used (Fig. 3B and fig. S8, B and C), suggesting that PEs alone do not effectively facilitate mucosal penetration. Similarly, when a SCOD was applied in the absence of PEs, relatively low d_p values were recorded (Fig. 3B and fig. S8D).

To better understand drug permeation at different degrees of mechanical stretching, we varied stretching forces by changing the pressure inside the SCOD. The SCOD was loaded with Cy5, PVA, and C10 and then connected to a vacuum pump capable of precisely controlling the pressure inside the patch (fig. S9). Deformation depended on negative pressure and correlated to the d_p values of 257 ± 163 μm, 799 ± 552 μm, and 5204 ± 302 μm at 0, −30, and − 50 kPa, respectively (Fig. 3C and fig. S10, A to C). When the SCOD was applied using manual compression (Fig. 3C and fig. S10D), a d_p of 4182 ± 420 μm was obtained, suggesting that the pressure inside the SCOD was around −50 kPa. This coincided with the observed SCOD adhesion force measurements between 40 and 60 kPa (fig. S3). Similar to the negative pressure effects described above, increasing the amount of PE (NaTaC) substantially increased d_p (Fig. 3D and fig. S11, A to D). Furthermore, both upscaling and downscaling of the SCOD dosage form did not reveal substantial differences in d_p (fig. S12, A to D), confirming the potential for adapting the patches to the individual patient's need, for example, smaller sizes for pediatric patients.

Next, we assessed the performance of the SCOD delivery technology in the presence of the PE NaTaC using a series of differing-Mw drug surrogates at three different application times (10 min, 30 min, and 3 hours). The data are compiled in Fig. 3E, and the microscopic fluorescence images for the various tested compounds at time points 10 min (fig. S13, A to E), 30 min (fig. S14, A to E), and 3 hours (fig. S15, A to E) are shown. As expected, with increasing application time, the d_p of all tested molecules increased because of the prolonged release from the polymer matrix and their time-dependent diffusion inside the tissue. When increasing the Mw of poly(ethylene glycol) (PEG)–modified Cy5 from 2k to 20k, a trend toward lower d_p could be observed. However, in the absence of a PE, 2k PEG-modified Cy5 penetrated deeper than Cy5 despite the Mw of 2k PEG-modified Cy5 being ~4 times higher than unmodified Cy5 (fig. S16). When the even larger and highly charged quantum dots (Q-dots) (carboxylic group–functionalized, Ø 5 nm) were tested, their d_p remained below 350 μm (depth of basal membrane).

In vivo pharmacokinetic study in beagle dogs

We then compared SCOD administration to intravenous injection and oral delivery with commercially available tablets of the peptide drug desmopressin in beagle dogs. Desmopressin (20 μg) was injected intravenously as a 5-ml bolus (Fig. 4A), whereas desmopressin tablets (1.2 mg) were administered orally after encapsulation in enteric capsules to avoid drug degradation in the stomach. The SCOD patch was first loaded with 1.2 mg of desmopressin and 1.2 mg of PVA and manually applied for 3 hours to the dog′s buccal mucosa. The average absolute oral bioavailability of the tablets was found to be 0.12% (n = 3), with the time required to reach a maximum plasma concentration of 1.2 hours (Fig. 4B), which is in line with previous values (*30*). Plasma concentrations of SCOD-delivered desmopressin gradually increased over the first 3 hours of application and peaked 4 hours after the start of the experiment (1 hour after SCOD removal) (Fig. 4B and tables S2 and S3). This may indicate a reservoir effect of the buccal epithelium similar to transdermal formulations (*31*). The calculated absolute bioavailability was 0.16% (n = 3), which was comparable to the desmopressin tablets.

In line with our ex vivo experiments, we then explored the synergistic effects of mechanical stretching and PE on drug absorption. The SCOD loaded with 1.2 mg of desmopressin and 2.1 mg of C10 (C10:desmopressin molar ratio of 10:1) increased the bioavailability by more than 10 times compared with the SCOD without C10, reaching 1.9% (Fig. 4C; n = 3). Although the bioavailability was higher, desmopressin formed a slowly dissolving complex with C10 (in vitro desmopressin release of about 30% after 3 hours; fig. S5D), leaving insoluble residues in the SCOD after in vivo application. Furthermore, the t_{max} was at 2.0 hours when C10 was included in the formulation (Fig. 4C). When changing the PE to NaTaC at the same molar ratio (10:1), a marked increase in absorption was achieved (Figs. 4D) (*29*). The desmopressin plasma concentrations were more than 150 times higher than after oral administration (Fig. 4, B and D), resulting in a bioavailability of 16.4% after a 3-hour patch application (n = 3). The NaTaC-related absorption enhancement allowed the reduction of SCOD application time from 3 hours to 10 min, which may be important for improving patient acceptability of the suction patch. After a 10- and 30-min application time, bioavailability was reduced to 3.2 and 4.1%, respectively, which was still 25 to 35 times higher than the marketed oral medication (Fig. 4D). To better decouple the contributions of mechanical stretching versus PE to the bioavailability, the experiment with NaTaC-loaded SCOD was repeated but in the absence of mechanical deformation (Fig. 4E). This was achieved by holding the SCOD to the mucosa with a clamp (0 kPa) for 30 min (fig. S6). In this scenario, the bioavailability (Fig. 4, F and G) fell to 0.12%, which was similar to SCOD without PE and oral desmopressin capsules.

To further validate the approach, the NaTaC-loaded SCOD performance was evaluated with another peptide drug, semaglutide, which has about four times higher Mw than desmopressin (4114 g/mol). The same molar ratio (1:10) was used with a 30-min SCOD application time. The pharmacokinetic profile of SCOD-administered semaglutide was compared with that of the oral Rybelsus tablet marketed in 2019. Rybelsus contains 9 mg (three times of 3-mg Rybelsus tablets) of semaglutide and has less than 1% bioavailability under strongly regulated intake instructions, taken at least 30 min before the first meal of the day and taken with less than 120 ml of water (*32*). The pharmacokinetic profile of 9 mg of semaglutide delivered via the SCOD over 30 min was nearly superimposable to that of Rybelsus (Fig. 4H). Moreover, interanimal variability was substantially decreased with the SCOD, as evidenced by a 52% reduction of the coefficient of variation for the area under the plasma concentration–versus–time curve ($AUC_{0–72}$) (table S4). More than 8 mg of semaglutide remained recoverable in the SCOD after application, meaning that less than 10% of the available semaglutide was accessed for diffusion within the 30-min application time frame (table S5).

In vivo safety evaluation

To evaluate the safety of the suction-based delivery method, the animal′s buccal mucosa was systematically photographed during the experiments. All patches adhered efficiently to the mucosa for 3 hours without falling off. In the absence of a PE, the SCOD minimally affected the tissue, with no signs of irritation and full apparent tissue recovery within 3 hours (fig. S17). Similarly, in the absence of mechanical stretching but with the PE, the mucosa showed no sign of irritation after 30-min application (fig. S18). More obvious swelling of the mucosa was observed under combined mechanical stretching and PE (C10 and NaTaC), over 3 hours, with full recovery achieved after a day or a week after application, respectively (figs. S19 and S20). For the 10- and 30-min applications, the addition of a PE induced slight swelling of the mucosal surface, which fully resolved within 6 to 24 hours after patch removal (Fig. 4I and figs. S21 to S23).

In a separate study, a small biopsy was taken at the application site 24 hours after the SCOD (including 5.7 mg of NaTaC) removal and at the symmetrical site on the other cheek of the dog. As shown in fig. S24, the buccal mucosa′s integrity was fully restored after 24 hours, without any visual or histological differences.

First-in-human study on the acceptance of the formulation

Last, we investigated SCOD patient acceptability and comfort in a first-in-human study. A drug- and PE-free patch (only loaded with water before application; fig. S25) was self-applied for 30 min to the buccal mucosa of 40 healthy volunteers between 24 and 63 years old (table S6). The same SCOD design tested in vivo (without drugs or excipients) was used for the first-in-human study but with slight modifications (fig. S2A). In this case, the patch was fabricated by

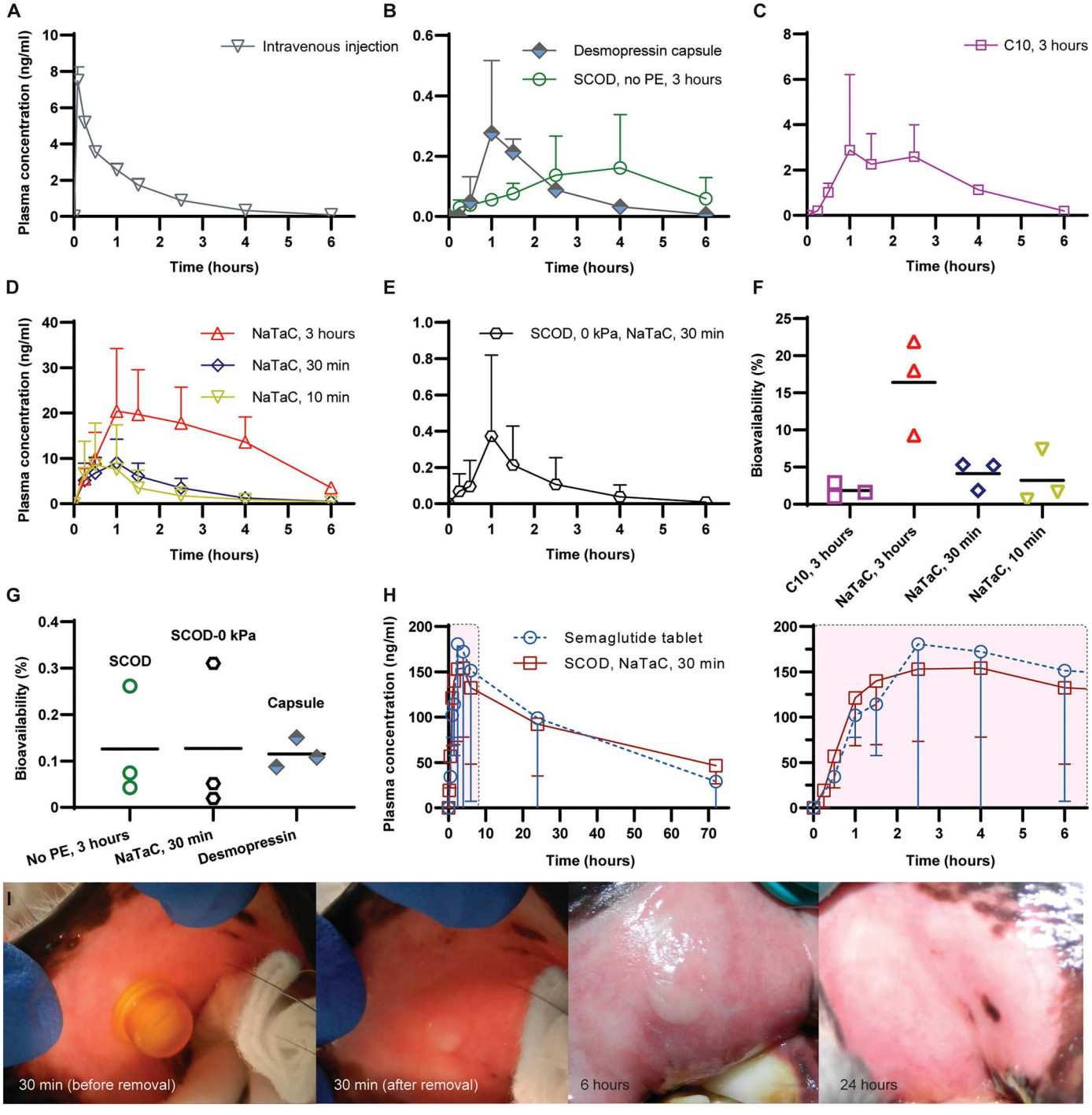

Fig. 4. Pharmacokinetic studies of desmopressin and semaglutide in beagle dogs. Plasma concentration of desmopressin after (**A**) a 5-ml bolus injection of 20 μg of desmopressin (Minirin), (**B**) oral administration of enteric encapsulated Minirin tablets (1.2 mg of desmopressin), or 3-hour application of SCOD loaded with 1.2 mg of desmopressin and 1.2 mg of PVA. (**C**) Three-hour application of the SCOD with the addition of 2.1 mg of C10. (**D**) Application of the SCOD loaded with 5.7 mg of NaTaC for 10 min, 30 min, and 3 hours. (**E**) Application of the same SCOD using an in-house–designed clamp (0 kPa) for 30 min. (**F** and **G**) Bioavailability (0 to 6 hours) of desmopressin from the formulations in (B) to (E). Detailed parameters are listed in tables S2 to S5. (**H**) Plasma concentration of semaglutide after oral administration of Rybelsus tablets (9 mg) or after 30-min application of SCOD loaded with 9 mg of semaglutide, 1.2 mg of PVA, and 11.7 mg of NaTaC. Right panel shows the pharmacokinetic profile during the first 6 hours. (**I**) Images of the buccal mucosa of a beagle dog 30 min, 6 hours, and 24 hours after application. Pharmacokinetics data are presented as means ± SD (n = 3). Solid black lines in (F) and (G) indicate mean bioavailability (n = 3).

a scalable mold-casting process using food-grade poly(dimethylsiloxane) (PDMS) (fig. S26, B to E). The mechanical properties (fig. S27A), ex vivo permeation-enhancing effects (fig. S27B), and adhesion strength (fig. S27C) of the food-grade PDMS patches were comparable to those of the ex vivo poly(β-thioether ester) construct. A small cylinder was added to the top of the SCOD to which dental floss could be attached and strung to an individual's shirt to avoid accidental swallowing (fig. S26F). Participants applied the suction patches themselves by compressing them onto the buccal region in the mouth with one finger counterbalancing from the outside (figs. S28, A and B, and S29, A to D). Once the patch was fully compressed and the fingers released, the SCOD firmly adhered to the mucosa. During the 30-min application time, the participants were allowed to talk, ambulate, and rinse their mouth with water without affecting the adhesion of the SCOD. Only five suction patches (12.5%) fell prematurely (two cases after 10- to 15-min application and three cases after 23- to 27-min application) because of suboptimal positioning (too close to the edges of the buccal region) or manipulating the patches.

An endoscopic camera was used to image the participants' buccal mucosa (figs. S29, A and B, and S30, A to C). The SCOD patch induced minimal alteration of the tissue upon which it was placed, and traces of the application were barely visible 1 hour after the removal (fig. S29B). A majority of participants (>92%) reported the application as generally comfortable to only mildly uncomfortable (fig. S29C). Only one participant indicated that the patch was uncomfortable. One hour after removing the patch, most of the participants (75%) reported feeling nothing unusual after the SCOD application. In all cases, participants could not distinguish the mucosal site where the SCOD was applied from normal mucosa 1 day after removal.

Participants were asked about their preferred drug administration route (needle injection, SCOD, or no preference) before test application (table S7). The majority communicated a clear preference toward SCOD for potential daily, weekly, and monthly applications (77.5, 72.5, and 57.5%, respectively). An hour after removing the patches, participants responded to the same questions again and indicated an increased preference toward the SCOD by 5.0% (daily), 17.5% (weekly), and 10.5% (monthly) (fig. S29D).

DISCUSSION

In this work, we developed a technology that can increase the absorption of peptide drugs. The design of our suction patches was bioinspired and mimicked the structure characteristic of octopus suckers, allowing both strong adhesion and mechanical deformation of the buccal mucosa (*33*). A negative pressure–based disruption has been previously explored for transdermal drug delivery using externally applied vacuum pumps (*34*, *35*). However, systemic absorption was low because of resilient stratified skin structures and mainly took place through the hair follicles (*36*). In comparison, the buccal epithelium is much thinner and lacks the keratinized cell layers, which could result in a more marked disruption of barrier functions.

Through a series of ex vivo experiments, we demonstrated a difference in tissue structures between unstretched and SCOD-stretched regions, which suggests a decreased mucosal barrier thickness upon mechanical stretching. The cellular responses to such mechanical forces were further examined with histological studies by staining F-actin, which is a characteristic marker of an intact inter- and intracellular structure. Because the phalloidin only binds to the polymerized F-actin and not to its monomeric form, G-actin, nor F-actin degradation products (*37*), the reduction in F-actin intensity observed in the presence of PE and suction implied a destabilization of its meshwork. Therefore, the cytoskeleton of the epithelial cells may be rearranged as it experiences simultaneous mechanical stretching and chemical PE stressors. Similar reversible rearrangements have been reported previously (*38*). It seems plausible that the mechanical stretching disrupts the mucosal barrier, promoting the diffusion of PE into the deeper cell layers. The synergism between mechanical stretching and chemical permeation enhancement throughout the mucosa allows for more efficient delivery of the drug surrogate.

In the ex vivo experiments on PEs, it should be noted that SNAC has been approved for semaglutide in the Rybelsus tablet, whereas pelargonidin was recently reported to substantially improve the absorption of insulin after oral administration (*39*). The lesser effectiveness of these two PEs compared with those of C10 and NaTaC on the buccal mucosa versus the intestinal mucosa implied that different mechanisms of action could be involved (*18*). Therefore, although a more than 20-fold increase of the d_p value was observed with NaTaC and C10 as compared with the separately applied mechanical and chemical methods (Fig. 3, A and B), there was a synergistic effect between the mechanical stretching and PEs. Furthermore, when using 2k PEG-modified Cy5 as a drug surrogate, we observed that it penetrated deeper than Cy5 despite the higher Mw. This suggests that besides Mw, other physiochemical properties, such as logP and charge, might influence permeation (*40*, *41*). Although further investigations are needed to confirm the exact Mw threshold of molecules that can be effectively delivered by this noninvasive method, we estimate an upper limit to be possibly in the range of 20 to 50 kDa.

The in vivo evaluation of the SCOD was carried out in beagle dogs because their buccal mucosa is nonkeratinized and similar to that of humans. The beagle therefore represents a good animal model for studying buccal absorption (*19*, *42*). Desmopressin (1189 g/mol) was selected as a model peptide because of its low oral bioavailability (<0.3%) and low plasma peak concentration in humans (~ 80 pg/ml) (*30*). The peptide has an isoelectric point of 10.2 and tends to be relatively quickly degraded in the GI tract. Our data demonstrated that the combination of PE and the SCOD markedly enhanced the bioavailability of desmopressin. Aside from mucosal stretching and chemical disruption, another factor that might further improve drug permeation is the protection of drugs within a SCOD during administration. Specifically, during SCOD application, drugs are confined and protected inside the patch, which helps maintain a high concentration gradient and close physical contact with the mucosal surface. In the case of semaglutide, we showed that more than 8 mg of the drug remained recoverable in the SCOD after removal, meaning that less than 10% of the available semaglutide was accessed for diffusion within the 30-min application time frame (table S5). This suggests that absorption might be improved by optimizing formulation parameters such as the dissolution rate, concentration gradient, PE concentration, time of application, and degree of mucosal deformation. These in vivo bioavailability results align with the ex vivo study data and demonstrate the benefit of combining mechanical stretching and PE to improve drug permeation/bioavailability. With the high tolerability

in the first-in-human study, this work suggests the potential for the SCOD's clinical translation.

However, as mentioned above, there are limitations to this study. First, only a limited number of PEs and PE doses were explored. Further efforts should be spent in the future to optimize the choice of the PE as well as its concentration to ensure both safety and efficacy. Compared with the oral route, PEs for the buccal mucosa have been much less explored, and their mechanisms of action have not been well characterized. Moreover, although the SCOD approach was less invasive than injections and the mucosa fully recovered within 24 hours after removal, the impact of repeated administration of the suction patches on the buccal mucosa still needs to be assessed. For the successful translation of the formulation, long-term safety and patient acceptance are of paramount importance.

In conclusion, the bioinspired SCOD technology presented here is noninvasive, simple, and readily self-applicable by patients. Its simplicity and modularity make this technology potentially suitable for administration of a wide range of compounds that are rapidly degraded or poorly absorbed in the GI tract. Furthermore, it could enable more efficient delivery of drugs that undergo extensive first-pass metabolism. Therefore, the SCOD technology could provide a realistic alternative to parenteral administration.

MATERIALS AND METHODS

Study design

This work aimed to develop a simple, safe, and noninvasive buccal drug delivery platform technology based on an octopus-inspired suction patch. The SCOD was designed to adhere to the buccal mucosa, mechanically stretch the tissue, and allow for the loading of a drug formulation. The patches were fabricated via 3D printing with a biocompatible polymer or via cast molding with a food-grade PDMS. Both materials were mechanically characterized ($n = 3$), and the cytotoxicity of the 3D-printed objects was tested. Ex vivo experiments on fresh porcine buccal tissue were carried out to measure the adhesion strength of the patch, evaluate the permeation-enhancing properties of formulations with drug surrogates, and investigate the permeation-enhancing mechanism ($n = 3$). In vivo pharmacokinetic studies were performed in beagle dogs ($n = 3$) with SCOD and control formulations (not randomized, no study size calculation, not blinded). Additionally, an in vivo safety study was conducted in beagle dogs ($n = 3$), where biopsy samples were taken 24 hours after the application to confirm the formulation's safety (no study size calculation). Last, a first-in-human comfort study of the SCOD patch without drugs and excipients was carried out with healthy volunteers ($n = 40$) to assess human individuals' acceptance of the dosage form (no study size calculation). Procedures involving the care and the use of beagle dogs for pharmacokinetic studies were reviewed and approved by the Institute National de la Recherche Scientifique (INRS) Institutional Animal Care and Use Committee (protocol: 2002-04) and performed according to the Canadian Council on Animal Care guidelines and policies. Procedures involving the care and the use of beagle dogs for the histological analysis were reviewed and approved by the Institutional Animal Care and Use Committee of the Shenzhen Advanced Medical Service Co., Ltd. (approval no. AAS200503D). The in-human study was approved by ETH Zurich Ethics Commission (2021-N-80) and conducted on a population of healthy volunteers at ETH Zurich.

Materials used

Hexane (≥97%), ethyl acetate (≥99.7%), phosphate-buffered saline (PBS), acetonitrile (ACN) (≥99.9%), sodium hydroxide (NaOH), SephadexLH-20, tris(hydroxymethyl)aminomethane (≥99.9%) (Trizma base, tris), CdTe core-type Q-dots (COOH functionalized), 2-propanol (isopropanol) (≥99.8%), bovine serum albumin (≥96%), Triton X-100, methanol-free paraformaldehyde (PFA), 2-methylbutane, diurethane dimethacrylate (DUDMA), (ethylenedioxy)diethanethiol (EDT), (+)-α-tocopherol (vitamin E), *N*-vinyl-2-pyrrolidone (NVP), phenylbis(2,4,6-trimethyl-benzoyl)-phosphine oxide (BAPO), 1-(phenyldiazenyl)naphthalen-2-ol (Sudan I), and (−)-riboflavin (≥98%) (vitamin B2) were purchased from Sigma-Aldrich. Methanol (Optima grade), ACN (Optima grade), formic acid [American Chemical Society (ACS) grade], glacial acetic acid (ACS grade), ammonium hydroxide (28%) (NH_4OH), nonyl β-D-glucopyranoside (NGP), phosphoric acid, Dulbecco's modified Eagle's medium (DMEM) with GlutaMAX (DMEM GlutaMAX), DMEM/F-12 Nutrition Mixture (with glutamine and 15 mM Hepes, without phenol red) (DMEM/F12), dimethylformamide (DMF), trypan blue solution 0.4%, antibiotic-antimycotic (100×) (10,000 U of penicillin, 10 mg of streptomycin, and 25 μg of amphotericin B per ml), trifluoroacetic acid, PBS for cell culture, and DMEM (without phenol red) were purchased from Thermo Fisher Scientific. Hoechst 33342 dye, ProLong Diamond Antifade Mountant, fetal bovine serum, 1% penicillin-streptomycin, and trypsin (0.25% + EDTA) were purchased from Invitrogen. Sodium decanoate (C10) (>99%) was purchased from Tokyo Chemical Industry. Ethanol (EtOH) absolute extra pure was purchased from Merck Millipore. Salcaprozate sodium (SNAC) was obtained from Fluorochem Ltd. Taurocholic acid sodium salt (≥98%) (NaTaC) was purchased from Roth AG. PEG-Cy5 (≥95%) (2k, 5k, and 20k) were purchased from Biopharma PEG Scientific. iFluor 488–conjugated phalloidin (ab176753) was purchased from Abcam. PDMS Bluesil RTV 3428 was purchased from Elkem. Optimal cutting medium (OCT) was purchased from Leica Microsystems. Pelargonidin chloride (≥97%) was purchased from Extrasynthesis. PVA 15k was purchased from Fluka. Triethylamine (≥99%) (TEA) and hydrogen peroxide (H_2O_2) 35% were purchased from Acros Chemicals. Hydrochloric acid was purchased from VWR. Methanol-d4 (CD_3OD) was purchased from Cambridge Isotope Laboratories. Desmopressin acetate (98%) was purchased from MuseChem. Semaglutide (acetate salt) (99%) was purchased from Career Henan Chemical. Sulfo–cyanine 5 free acid (Cy5) was purchased from Lumiprobe GmbH. Eudragit L100-55 was provided by Evonik. Desmopressin tablets (0.2 mg, Minirin) and desmopressin injection solution (4 μg/ml, Minirin) were purchased from FERRING Arzneimittel GmbH. Semaglutide tablets (3 mg, Rybelsus) were purchased from Novo Nordisk. Goserelin acetate (88.6% peptide content) was purchased from Bachem. Sylgard 184 silicone elastomer kit was purchased from Dow. Xylazine hydrochloride was purchased from Dunhua Shenda Animal Pharmaceuticals Co. Ltd. Neutral buffered formalin (10%) was purchased from Macklin Inc. Chemicals for hematoxylin and eosin staining: Mayers hematoxylin, eosin solution, EtOH, PBS, and xylene were purchased from Wuhan Servicebio Technology Co., Ltd.

Polymer and resin preparation

DUDMA (60 g) was dissolved in extra dry DMF (120 ml). EDT (20.75 ml) and TEA (12 ml) were then added while stirring, followed by the addition of vitamin E (300 mg). The mixture was left at 80°C for 4 days under constant stirring (400 rpm) and then slowly cooled down to room temperature (RT). The resulting polymer was washed three times with 150 ml of an ethyl acetate/hexane mixture [ethyl acetate:hexane ratio was 1:1, 1:3, and 1:5 (v/v), respectively], and the supernatant was discarded. The viscous liquid was then washed twice with hexane (200 ml), and solvent residues were removed by drying the product at 60°C in a rotary evaporator under reduced pressure to afford poly(β-thioether ester) polymer (yield: 72 ± 4 g, 78 to 87%). The polymer was characterized by ^{1}H nuclear magnetic resonance spectroscopy (AV400, Bruker) using CD_3OD as a solvent.

To prepare the resin, 14 g of poly(β-thioether ester) polymer was added to a brown glass vial. Then, 132 mg of BAPO (0.94 wt %), 6 mg of Sudan I (0.04 wt %), and 10 mg of vitamin E (0.07 wt %), previously dissolved in 4.5 ml (30.9 wt %) of NVP, were added to the vial. The resin was heated to 80°C under mixing and then sonicated (Bandelin Sonorex, Bandelin electronic GmbH & Co. KG) at 80°C for at least 2 hours until a homogeneous mixture was obtained.

Digital light processing 3D printing of suction patches

Suction patches were designed using the SolidWorks program (Dassault Systèmes) (Fig. 1) and converted to an STL format. The designs were processed for printing with the Asiga Composer (Version 1.2) software (Asiga). Last, suction patches were 3D printed by using a commercial digital light processing 3D printer (Asiga PICO 2, Asiga) with a customized resin tray and a printing head with heating functions as described in detail previously (*23*). The printing was performed at 90°C, with an exposure time of 4.0 s and an initial exposure time of 35 s. After printing, the objects were cleaned with 2-propanol and then cured in an ultraviolet chamber (Asiga Pico Flash, Asiga) for 5 min (each side) from the top and the bottom. For tensile tests, dog bone–shaped specimens were 3D printed and tested at a rate of 6 mm/min using a TA.3DXTplus texture analyzer (Stable Micro Systems) with a 50-N load cell.

Tissue preparation for ex vivo analysis

Freshly extracted porcine buccal tissue (animal age: 5 to 6 months, weight: 100 to 120 kg) was obtained from the local slaughterhouse (Schlachtbetrieb Zürich AG) and immediately immersed in DMEM/F12 medium containing 1% (v/v) antibiotic-antimycotic (100×) and placed on ice within 15 min. No later than 2 hours after extraction, the cheek was processed by removing excess skin, fat, and muscle tissue to trim it to a thickness of ~1.5 to 2 cm. The tissue was cut into pieces without damaging the mucosa to fit into a six-well plate (TPP) and incubated in DMEM/F12 medium for ~20 min at 37°C before application to suction patches for penetration depth or adhesion measurements.

Clamp design and application ex vivo

The clamp was designed in a way that the suction patch can be applied without negative pressure to avoid tissue deformation while preserving similar application conditions including no drug dilution and same contact area. The clamp was designed using the program Solidworks and then 3D printed (Prusa i3 MK3, Prusa Research) with poly(lactic acid) (PLA) filament (Extrudr PLA NX2, FD3D GmbH) in the ETH Zurich mechanic shop. A common screw was modified by hand to allow clip insertion of the screw's tip into a housing on top of the counter plate to provide flexibility with tissue fixation. The assembled clamp is shown in fig. S6. The suction patch was prepared as described above and placed into the cavity at the bottom of the clamp's main body. Immediately before application, the patch was loaded with 120 μl of deionized (DI) water, and the porcine cheek (mucosa facing the suction patch opening) was placed between the suction patch and counter plate. After the correct positioning of the tissue, the screw was tightened, and spilled drug surrogate formulation was removed with PBS. Subsequently, the sample was placed in a petri dish (TPP), filled with DMEM/F12, and incubated for 3 hours at 37°C. To remove the suction patch at the end of the experiment, the screw was untightened, and the tissue was gently removed and further processed as manually applied suction patches (see section "Suction patch loading with surrogate and application ex vivo").

Controlled negative pressure device

The device was constructed to allow precise and continuous negative pressure control inside the suction patch by creating a hypobaric pressure inside the system. A schematic representation and images of the final setup are shown in fig. S9. The electric power supply (fig. S9A, yellow) powered a vacuum pump (fig. S9B, red) (SP 270 EC, 12 Vdc, Schwarzer Precision GmbH) that created a constant negative pressure of up to 50 to 60 kPa. Because of the adjustability of the air inflow by the reduction valve (fig. S9C, purple) (SO NV 51D21-6, Serto AG), the negative pressure in the system was precisely regulatable. The pressure value inside the system was monitored and logged live (1 measurement/s) by a pressure sensor (fig. S9D, green) (UPS-HSR-B02P5G, Stork Solutions Ltd) by a computer. A 3D-printed (Asiga PICO 2) suction patch holder (3×) was mounted at the end of the system onto a tubing, which was guided into an incubator (37°C) (WTC Binder) to perform the experiment at 37°C (fig. S9E, orange). A perforated (<1-mm Ø hole on top of the suction patch's dome) and formulation-loaded (as described above) suction patch was placed into the holder (patch opening facing away from the holder). The contact area between the holder and the suction patch was sealed with a dental cream (Candida, Migros).

Suction patch loading with surrogate and application ex vivo

Cy5 (final concentration, 2 mM) 2k (2 mM), 5k (2 mM), and 20k (1 mM) PEG-Cy5 or Q-dots (2 mg/ml) were dissolved in DI water containing 3 wt % 15k PVA. Subsequently, PE (C10, NaTaC, pelargonidin chloride, or SNAC) was added to obtain a final concentration of 0 to 265 mM. The suction patches were loaded with 40 μl of solution via drop casting (fig. S5) and allowed to dry overnight under ambient conditions, followed by drying under vacuum for 1 hour at RT. To apply them onto the porcine mucosa, the patches were loaded with 80 μl of DI water and immediately compressed by hand onto the mucosa. Spillovers that leaked during compression were rinsed off with PBS. Then, the tissue with the suction patch was placed in a six-well plate (TPP), and the tissue was covered with fresh, prewarmed DMEM/F12 and incubated at 37°C from 10 min to 3 hours. After the incubation, the suction patch was removed by letting air in at the rim to break the seal, and the tissue was gently rinsed with PBS.

For the application of the suction patch under controlled negative pressure conditions, the negative pressure device (designed in-house, see above) was used. The patch was loaded with 80 μl of DI water and placed onto the mucosa in a six-well plate by hand. With the correct positioning of the suction patch, the vacuum pump was turned on, and the pressure was adjusted to 30 or 50 kPa below atmospheric pressure. Subsequently, the tube connected to the suction patch holder was fixed in place, and the well containing the tissue was filled up with fresh, prewarmed DMEM/F12 medium. During the incubation period of 3 hours at 37°C, the pressure was frequently readjusted to keep it in a range of ±5 kPa. Last, the pump was turned off and the system was ventilated, allowing the immediate detachment of the suction patch.

Within 1 min after suction patch removal, the sample was cryopreserved by snap freezing in a liquid nitrogen–chilled isopentane bath for ~1 min. Last, the sample was embedded in an optimal cutting medium (OCT) and stored at −20°C until further imaging or immunohistology studies within 2 weeks.

Suction patch loading with desmopressin or semaglutide

Desmopressin was dissolved in DI water containing 3 wt % 15k PVA. PE (C10 or NaTaC) was then added to achieve the final concentration of 26.5 mM for desmopressin, 265 mM for PE, and 2 mM for PVA. The solution was vortexed, and the suction patches were loaded in the same way as described above for surrogate formulations, resulting in ~1.2 mg of desmopressin per patch.

For semaglutide, a fresh tris-HCl buffer with a pH of 7.4 and an osmolality of 280 mOsmol/kg was prepared. Semaglutide was then dissolved in tris-HCl buffer containing 1.5 wt % 15k PVA followed by the addition of NaTaC up to the final concentration of 27.35 mM for semaglutide, 273.5 mM for NaTaC, and 1 mM for PVA. The solution was vortexed, and the suction patches were loaded with 80 μl in the same way as described above for surrogate formulations, resulting in ~9 mg of semaglutide per patch.

Sample preparation and imaging parameters for penetration depth quantification

Sectioning of the cryopreserved ex vivo samples was conducted by using the cryostat (CryoStar NX50, Thermo Fisher Scientific). During sectioning, the temperature was kept at −20°C. The thickness was set to 20 μm. To prevent photobleaching of the fluorescent marker, the light in the room was reduced to a minimum. The samples were thawed for 30 min at RT. Afterward, they were incubated for 5 min in freshly prepared 4% methanol-free PFA in PBS and washed in PBS for 3 min. Sample slides were then mounted with ProLong Diamond Antifade Mountant and a coverslip. Fluorescent images of the sections were taken using the Leica DMI 6000 B microscope with adaptive focus control (annual maintenance by Leica support service, Leica Microsystems) at a magnification of ×20 [HC PL FLUOTAR L 20x, with correction collar (CORR), numerical aperture: 0.4, dry, Leica Microsystems] using the LAS X software (Leica Microsystems) in the tile scan mode (manual and automatic focusing; range, 60 μm) and were merged afterward. Light was emitted by an EL6000 mercury metal halide bulb (Leica Microsystems). Images were detected by monochrome DFC365FX digital camera (12 bits, 1 × 1 BIN, Leica microsystems). For Cy5 as well as Cy5-labeled PEG, the Y5 channel [excitation (EX), 590 to 650 nm; dichroic mirror (DC), 660; emission (EM), 662 to 738 nm; product number (PN), 11504203] and for the Q-dots, the TxR channel (EX, 542 to 582 nm; DC, 593; EM, 604 to 644 nm; PN, 11504207) was used. The gain was kept at 2 to 5 and the exposure time < 300 ms. The gain and exposure time were confirmed to be linear in the measurement range and adjusted to avoid overexposure of the scans.

For histology evaluation, the samples were imaged with the same system at a magnification of ×40 (HXC PL FL 40×/0.75, with CORR, numerical aperture: 0.4, dry, Leica Microsystems) in the tile scan mode and merged afterward. Three channels per frame were used, Y5 for Cy5 (EX, 590 to 650 nm; DC, 660; EM, 662 to 738 nm), L5 for Phalloidin-conjugated iFluor 488 (EX, 460 to 500 nm; DC, 505; EM, 512 to 542 nm; PN, 11504166), and A4 for Hoechst 33342 (EX, 340 to 380 nm; DC, 400; EM, 450 to 490 nm).

Penetration depth (d_p) quantification

The analysis of the surrogate′s penetration depth is based on the fluorescence microscopy images. Only the central part (region of deformation) was used for quantification. Image analysis was carried out using ImageJ (National Institutes of Health) in the grayscale mode, with a pixel depth of 0 to 4095 representing the fluorescence intensity by directly importing the raw (.lif) file. Straight line profiles with a width of 300 pixels and 4- to 7-mm length were obtained vertically to the mucosa surface. Each measurement generated a line profile with the average fluorescence intensity as a function of the distance. Every scan was measured five times at different positions. Furthermore, the background signal (noise by autofluorescence) was measured by a line profile analysis at the bottom of the tissue (parallel to the mucosa) with the length of the entire cross-section. Generated intensity profiles were transferred to a Microsoft Excel template sheet for further data processing (see data files S1 and S2).

To evaluate the penetration depth by absolute fluorescence intensity, first, all intensity values were normalized to the same gain and exposure time. Second, the average baseline intensity plus three times its SD was defined as cutoff value [0 arbitrary units (a.u.)] to correct for autofluorescence and background noise. Third, the data were processed with MATLAB (MathWorks Inc.). There, the cutoff value was subtracted from the obtained intensities. Afterward, the x value (distance) that corresponded to the highest y value (absolute fluorescence intensity) was defined as new 0 distance because the maximum intensity is expected to be found on the epithelium′s surface (see data file S3). Next, the d_p was set to the first value below a threshold intensity of 50 or 20 a.u. If within the next 300 μm (corresponding to 650 data points) the intensity increased above the threshold for at least 300 μm, a new d_p was set at the next value below the threshold intensity (see data file S4). The resulting x value represents the penetration depth. Last, for each profile, obtained average values (n = 5 measurements) were plotted in GraphPad Prism 9 according to the test condition and statistically analyzed by a one-way analysis of variance (ANOVA) with Tukey′s comparison test ($\alpha = 0.05$): $P > 0.05$ [ns (not significant)], $^{*}P < 0.05$, $^{**}P < 0.01$, and $^{***}P < 0.001$.

Desmopressin pharmacokinetics

In vivo pharmacokinetic experiments were conducted at the INRS (CNBE, Laval, QC, Canada). Three beagle dogs (26 to 35 months) with body weights around 10 ± 1 kg were used.

Suction patches were prepared as described above and loaded with 1.2 mg of desmopressin and 1.2 mg of PVA and with or

without PE (2.1 mg of C10 or 5.7 mg of NaTaC). The dogs (fasted for 16 hours) were anesthetized during the duration of the patch application (10 min, 30 min, or 3 hours). The device was applied by manual compression and remained firmly in place for the time intended. For the control experiment without negative pressure, the clamp setup was used and applied to the dogs′ buccal mucosa. Blood samples were withdrawn at the indicated time points—0, 15, 30, 60, 90, 150, 240, and 360 min from start of patch application—and collected in K_2EDTA tubes (Bioreclamation IVT) followed by centrifugation at 1700*g* for 10 min at 4°C. Subsequently, the plasma was stored at −80°C until further analysis. Images were taken at different time points during patch application and after patch removal: 0 to 6 days after the start of experiment.

For oral administration, six Minirin tablets (the tablet form of desmopressin, 0.2 mg of desmopressin per tablet) were placed in a gelatin capsule and then enteric coated with Eudragit L100-55. An Eudragit L100-55 stock solution with a 14.3% (w/v) concentration was prepared using 100 ml of isopropanol together with 100 mg of vitamin B2 as a colorant to visualize the homogeneity of the solution. The coating was performed in a two-step dip coating method. The bottom part of the capsule was first immersed in the solution, lifted, and hung on a string until fully dried. The upper part was then immersed, and the capsule was then hung upside down until all solvents were completely evaporated. The dip coating procedure was repeated three times. Before drug administration, the dogs were fasted for 16 hours, and then two capsules containing in total 1.2 mg of desmopressin were orally given to the dog. Blood samples were withdrawn at indicated time points: 0, 30, 60, 90, 150, 240, and 360 min after oral application. Blood samples were collected in K_2EDTA tubes (Bioreclamation IVT) immediately followed by centrifugation at 1700*g* for 10 min at 4°C. Subsequently, the plasma was stored at −80°C until further analysis.

Intravenous injection

The intravenous administration was performed via the saphenous vein (left or right). The site was shaved and then cleaned using isopropyl alcohol (70%) (Greenfield Global). An IV catheter (Catheter IV Sur-Vet Teflon 22G × 1 in – Blue, Terumo) was inserted into the vein and secured using Transpore tape (The Steven Company). The desmopressin injection solution (4 μg/ml, Minirin) was administered using a 10-ml syringe (Betcon Dickison Canada Inc.) affixed with a 20G × 1 needle (Becton Dickison Canada Inc.) over a 1-min injection. After the administration, 250 μl of physiological saline (Baxter Corporation) was injected to flush the dead volume of the catheter.

Semaglutide pharmacokinetics

Suction patches were prepared as described above and loaded with 9 mg of semaglutide, 1.2 mg of PVA, ~ 1 mg of tris-HCl, and 11.7 mg of NaTaC. The dogs were anesthetized for the duration of the patch application (30 min). The device was applied manually and remained firmly in place for 30 min. For the commercial tablet control, in total three Rybelsus tablets (each with 3 mg of semaglutide) containing 9 mg of semaglutide in total were orally given to each dog that had fasted for 16 hours. Blood samples were withdrawn at indicated time points: 0, 15, 30, 60, 90, 150, 240, 360, 1440 (24 hours), and 4320 min (72 hours) after oral application and collected in K_2EDTA tubes (Bioreclamation IVT) followed by centrifugation at 1700*g* for 10 min at 4°C. Subsequently, the plasma was stored at −80°C until further analysis. Images were taken at different time points: 0 to 24 hours after the start of experiment.

Desmopressin plasma concentration analysis

The drug plasma concentration was evaluated using liquid chromatography–tandem mass spectrometry (LC-MS/MS) at the University of Montreal (Platform of Biopharmacy, Faculty of Pharmacy). Two calibration curves were obtained before and after the analytical batch in the range of 10 to 200 pg/ml. Desmopressin extraction from dog plasma samples was carried out by weak anion-exchange solid-phase extraction (SPE). More specifically, the samples were thawed, and an aliquot of 1000 μl of the dog plasma was then mixed with 10 μl of the internal standard (goserelin; final concentration, 25 ng/ml) and 300 μl of 4% (v/v) H_3PO_4-acidified water in a 1.5-ml Eppendorf tube (Fisher Scientific). The samples were then loaded into SPE cartridges (Strata-CW SPE cartridges 30 mg/1 cm^3, 30 μm, Phenomenex) preconditioned with 1 ml of methanol and 1 ml of purified water (Milli-Q ultrapure, Millipore) and aspirated by low vacuum. The cartridge was washed with 1 ml of a 4% (v/v) NH_4OH in 40:60 (v/v) ACN/water mixture. Afterward, the sample was eluted using 1 ml of methanol containing 5% (v/v) glacial acetic acid into 12-mm by 75-mm borosilicate glass tubes (Waters) that were placed in a 45°C water bath. A constant nitrogen gas flow for 12 to 20 min was applied to evaporate the solvents. The samples were reconstituted in 120 μl of 11:11:78 (v/v/v) ACN/methanol/DI water containing 1% (v/v) formic acid and 0.04% (v/v) NGP and mixed by vortexing. Subsequently, samples were transferred into 96-well V-bottom propylene plates (Waters) and centrifuged at 4883 rcf for 5 min. Last, 18 μl was injected into the Xevo G2 XS (Waters) equipped with an Acquity UPLC BEH C18 (50 mm by 2.1 mm, 1.7 μm) column (Waters). The analysis was carried out with a gradient of A [water + 0.2% (v/v) acetic acid] and B [ACN + 0.2% acetic acid (v/v)]: 1.5 min at 4% (v/v) B and then 4 to 50% (v/v) B within 2 min, at a flow rate of 0.4 ml/min at 60°C. Samples were ionized by electrospray ionization in the positive mode and analyzed in time-of-flight multiple-reaction-monitoring (TOF-MRM) mode with a lower limit of quantification (LLOQ) of <15 pg/ml. The LLOQ was defined as the lowest calibrator within ±30% of the nominal concentration. Results were transferred with the according sample code.

Semaglutide plasma concentration analysis

The drug plasma concentration was evaluated using LC-MS/MS at the University of Montreal (Platform of Biopharmacy, Faculty of Pharmacy). Two calibration curves in dog plasma were obtained before and after the analytical batch in the range of 8 to 400 ng/ml. The plasma samples were thawed on ice and kept at RT during the sample preparation. The plasma samples were extracted by protein precipitation before analysis. In brief, 40 μl of plasma was pipetted in a 1.5-ml polypropylene Eppendorf tube. The plasma was precipitated with two times its volume (80 μl) of an organic solvent solution consisting of ACN:methanol [80:20 (v/v)]. Samples were vortex mixed and centrifuged at 15870 rcf. Supernatant (90 μl) was further diluted with 60 μl of water containing 0.1% (v/v) formic acid (final dilution factor of 5×). The sample extracts were transferred into a 96-well plate. Last, 15 μl was injected into the Xevo G2 XS (Waters) equipped with an Acquity UPLC Protein BEH C4 (300A, 50 mm by 2.1 mm, 1.7 mm) column (Waters). The analysis was carried out with a gradient of A [water + 0.2% (v/v) formic acid] and B (ACN + 0.2% formic acid): 0.3 min at

20% (v/v) B and then to 50% (v/v) B within 5 min, at a flow rate of 0.3 ml/min and at 60°C. Samples were ionized by electrospray ionization in the positive mode and analyzed in TOF-MRM mode with a LLOQ of <8 ng/ml. The LLOQ was defined as the lowest calibrator within ±30% of the nominal concentration. The calibration curves were plotted using the peak area of the analyte, using a quadratic regression with a $1/x$ weighting factor. Results were transferred with the according sample code.

Statistical analysis

Statistical significance in cytotoxicity experiments between the 3D-printed object and the negative control sample, in various penetration depth analyses at given threshold values within one group, and in the bioavailability study of desmopressin was calculated by a one-way ANOVA with Tukey's comparison test ($\alpha = 0.05$): $P > 0.05$ (ns), $^{*}P < 0.05$, $^{**}P < 0.01$, and $^{***}P < 0.001$.

Supplementary Materials

This PDF file includes:
Figs. S1 to S30
Tables S1 to S7

Other Supplementary Material for this manuscript includes the following:
Data files S1 to S4
MDAR Reproducibility Checklist

REFERENCES AND NOTES

1. H. Rosen, T. Abribat, The rise and rise of drug delivery. *Nat. Rev. Drug Discov.* **4**, 381–385 (2005).
2. T. M. Allen, P. R. Cullis, Drug delivery systems: Entering the mainstream. *Science* **303**, 1818–1822 (2004).
3. D. J. Drucker, Advances in oral peptide therapeutics. *Nat. Rev. Drug Discov.* **19**, 277–289 (2020).
4. E. Moroz, S. Matoori, J.-C. Leroux, Oral delivery of macromolecular drugs: Where we are after almost 100 years of attempts. *Adv. Drug Deliv. Rev.* **101**, 108–121 (2016).
5. D. J. Brayden, T. A. Hill, D. P. Fairlie, S. Maher, R. J. Mrsny, Systemic delivery of peptides by the oral route: Formulation and medicinal chemistry approaches. *Adv. Drug Deliv. Rev.* **157**, 2–36 (2020).
6. S. T. Buckley, T. A. Bækdal, A. Vegge, S. J. Maarbjerg, C. Pyke, J. Ahnfelt-Rønne, K. G. Madsen, S. G. Schéele, T. Alanentalo, R. K. Kirk, B. L. Pedersen, R. B. Skyggebjerg, A. J. Benie, H. M. Strauss, P.-O. Wahlund, S. Bjerregaard, E. Farkas, C. Fekete, F. L. Søndergaard, J. Borregaard, M.-L. Hartoft-Nielsen, L. B. Knudsen, Transcellular stomach absorption of a derivatized glucagon-like peptide-1 receptor agonist. *Sci. Transl. Med.* **10**, eaar7047 (2018).
7. S. Tuvia, J. Atsmon, S. L. Teichman, S. Katz, P. Salama, D. Pelled, I. Landau, I. Karmeli, M. Bidlingmaier, C. J. Strasburger, D. L. Kleinberg, S. Melmed, R. Mamluk, Oral octreotide absorption in human subjects: Comparable pharmacokinetics to parenteral octreotide and effective growth hormone suppression. *J. Clin. Endocrinol. Metab.* **97**, 2362–2369 (2012).
8. M. Sakagami, Insulin disposition in the lung following oral inhalation in humans: A meta-analysis of its pharmacokinetics. *Clin. Pharmacokinet.* **43**, 539–552 (2004).
9. H. R. Costantino, L. Illum, G. Brandt, P. H. Johnson, S. C. Quay, Intranasal delivery: Physicochemical and therapeutic aspects. *Int. J. Pharm.* **337**, 1–24 (2007).
10. Y. Zhang, J. Yu, A. R. Kahkoska, J. Wang, J. B. Buse, Z. Gu, Advances in transdermal insulin delivery. *Adv. Drug Deliv. Rev.* **139**, 51–70 (2019).
11. N. C. Fay, B.-P. Muthusamy, L. P. Nyugen, R. C. Desai, A. Taverner, J. MacKay, M. Seung, T. Hunter, K. Liu, A. Chandalia, M. P. Coyle, H. L. Kim, S. Postlethwaite, K. Mangat, L. Song, E. Seto, A. Alam, C. V. Olson, W. Feng, M. Saberi, T. A. Mahmood, R. J. Mrsny, A novel fusion of IL-10 engineered to traffic across intestinal epithelium to treat colitis. *J. Immunol.* **205**, 3191–3204 (2020).
12. T. A. Al-Hilal, F. Alam, Y. Byun, Oral drug delivery systems using chemical conjugates or physical complexes. *Adv. Drug Deliv. Rev.* **65**, 845–864 (2013).
13. Z. Luo, N. Paunović, J.-C. Leroux, Physical methods for enhancing drug absorption from the gastrointestinal tract. *Adv. Drug Deliv. Rev.* **175**, 113814 (2021).
14. A. Abramson, E. Caffarel-Salvador, V. Soares, D. Minahan, R. Y. Tian, X. Lu, D. Dellal, Y. Gao, S. Kim, J. Wainer, J. Collins, S. Tamang, A. Hayward, T. Yoshitake, H.-C. Lee, J. Fujimoto, J. Fels, M. R. Frederiksen, U. Rahbek, N. Roxhed, R. Langer, G. Traverso, A luminal unfolding microneedle injector for oral delivery of macromolecules. *Nat. Med.* **25**, 1512–1518 (2019).
15. A. Abramson, E. Caffarel-Salvador, M. Khang, D. Dellal, D. Silverstein, Y. Gao, M. R. Frederiksen, A. Vegge, F. Hubálek, J. J. Water, A. V. Friderichsen, J. Fels, R. K. Kirk, C. Cleveland, J. Collins, S. Tamang, A. Hayward, T. Landh, S. T. Buckley, N. Roxhed, U. Rahbek, R. Langer, G. Traverso, An ingestible self-orienting system for oral delivery of macromolecules. *Science* **363**, 611–615 (2019).
16. W. Chen, J. Wainer, S. W. Ryoo, X. Qi, R. Chang, J. Li, S. H. Lee, S. Min, A. Wentworth, J. E. Collins, S. Tamang, K. Ishida, A. Hayward, R. Langer, G. Traverso, Dynamic omnidirectional adhesive microneedle system for oral macromolecular drug delivery. *Sci. Adv.* **8**, eabk1792 (2022).
17. A. K. Dhalla, Z. Al-Shamsie, S. Beraki, A. Dasari, L. C. Fung, L. Fusaro, A. Garapaty, B. Gutierrez, D. Gratta, M. Hashim, K. Horlen, P. Karamchedu, R. Korupolu, E. Liang, C. Ong, Z. Owyang, V. Salgotra, S. Sharma, B. Syed, M. Syed, A. T. Vo, R. Abdul-Wahab, A. Wasi, A. Yamaguchi, S. Yen, M. Imran, A robotic pill for oral delivery of biotherapeutics: Safety, tolerability, and performance in healthy subjects. *Drug Deliv. Transl. Res.* **12**, 294–305 (2022).
18. S. Şenel, A. A. Hıncal, Drug permeation enhancement via buccal route: Possibilities and limitations. *J. Control. Release* **72**, 133–144 (2001).
19. A. H. Shojaei, Buccal mucosa as a route for systemic drug delivery: A review. *J. Pharm. Pharm. Sci.* **1**, 15–30 (1998).
20. G. Campisi, C. Paderni, R. Saccone, O. Fede, A. Wolff, L. Giannola, Human buccal mucosa as an innovative site of drug delivery. *Curr. Pharm. Des.* **16**, 641–652 (2010).
21. B. M. A. Silva, A. F. Borges, C. Silva, J. F. J. Coelho, S. Simões, Mucoadhesive oral films: The potential for unmet needs. *Int. J. Pharm.* **494**, 537–551 (2015).
22. S. Hu, X. Pei, L. Duan, Z. Zhu, Y. Liu, J. Chen, T. Chen, P. Ji, Q. Wan, J. Wang, A mussel-inspired film for adhesion to wet buccal tissue and efficient buccal drug delivery. *Nat. Commun.* **12**, 1689 (2021).
23. J. Smart, The basics and underlying mechanisms of mucoadhesion. *Adv. Drug Deliv. Rev.* **57**, 1556–1568 (2005).
24. F. Veuillez, Y. N. Kalia, Y. Jacques, J. Deshusses, P. Buri, Factors and strategies for improving buccal absorption of peptides. *Eur. J. Pharm. Biopharm.* **51**, 93–109 (2001).
25. W. M. Kier, A. M. Smith, The morphology and mechanics of octopus suckers. *Biol. Bull.* **178**, 126–136 (1990).
26. F. McCartney, J. P. Gleeson, D. J. Brayden, Safety concerns over the use of intestinal permeation enhancers: A mini-review. *Tissue Barriers* **4**, e1176822 (2016).
27. C. E. Hoyle, C. N. Bowman, Thiol-ene click chemistry. *Angew. Chem. Int. Ed. Engl.* **49**, 1540–1573 (2010).
28. N. Paunović, Y. Bao, F. B. Coulter, K. Masania, A. K. Geks, K. Klein, A. Rafsanjani, J. Cadalbert, P. W. Kronen, N. Kleger, A. Karol, Z. Luo, F. Rüber, D. Brambilla, B. von Rechenberg, D. Franzen, A. R. Studart, J.-C. Leroux, Digital light 3D printing of customized bioresorbable airway stents with elastomeric properties. *Sci. Adv.* **7**, eabe9499 (2021).
29. H. P. Merkle, G. Wolany, Buccal delivery for peptide drugs. *J. Control. Release* **21**, 155–164 (1992).
30. T. W. Leonard, J. Lynch, M. J. McKenna, D. J. Brayden, Promoting absorption of drugs in humans using medium-chain fatty acid-based solid dosage forms: GIPET. *Expert Opin. Drug Deliv.* **3**, 685–692 (2006).
31. M. S. Roberts, S. E. Cross, Y. G. Anissimov, Factors affecting the formation of a skin reservoir for topically applied solutes. *Skin Pharmacol. Physiol.* **17**, 3–16 (2004).
32. S. Hughes, J. J. Neumiller, Oral semaglutide. *Clin. Diabetes* **38**, 109–111 (2020).
33. S. Baik, D. W. Kim, Y. Park, T.-J. Lee, S. Ho Bhang, C. Pang, A wet-tolerant adhesive patch inspired by protuberances in suction cups of octopi. *Nature* **546**, 396–400 (2017).
34. E. O. Lallow, N. C. Jhumur, I. Ahmed, S. B. Kudchodkar, C. C. Roberts, M. Jeong, J. M. Melnik, S. H. Park, K. Muthumani, J. W. Shan, J. D. Zahn, D. I. Shreiber, J. P. Singer, Y. K. Park, J. N. Maslow, H. Lin, Novel suction-based in vivo cutaneous DNA transfection platform. *Sci. Adv.* **7**, eabj0611 (2021).
35. F. Benaouda, R. Inacio, C. H. Lim, H. Park, T. Pitcher, M. A. Alhnan, M. M. S. Aly, K. T. Al-Jamal, K.-L. Chan, R. P. Gala, D. Sebastia-Saez, L. Cui, T. Chen, J. Keeble, S. A. Jones, Needleless administration of advanced therapies into the skin via the appendages using a hypobaric patch. *Proc. Natl. Acad. Sci. U.S.A.* **119**, e2120340119 (2022).
36. R. Inacio, S. Poland, X. J. Cai, S. J. Cleary, S. Ameer-Beg, J. Keeble, S. A. Jones, The application of local hypobaric pressure - A novel means to enhance macromolecule entry into the skin. *J. Control. Release* **226**, 66–76 (2016).
37. A. M. Lengsfeld, I. Löw, T. Wieland, P. Dancker, W. Hasselbach, Interaction of phalloidin with actin. *Proc. Natl. Acad. Sci. U.S.A.* **71**, 2803–2807 (1974).
38. H. Lin, M. Gebhardt, S. Bian, K. A. Kwon, C.-K. Shim, S.-J. Chung, D.-D. Kim, Enhancing effect of surfactants on fexofenadine·HCl transport across the human nasal epithelial cell monolayer. *Int. J. Pharm.* **330**, 23–31 (2007).

39. N. G. Lamson, K. C. Fein, J. P. Gleeson, A. N. Newby, S. Xian, K. Cochran, N. Chaudhary, J. R. Melamed, R. L. Ball, K. Suri, V. Ahuja, A. Zhang, A. Berger, D. Kolodieznyi, B. F. Schmidt, G. L. Silva, K. A. Whitehead, The strawberry-derived permeation enhancer pelargonidin enables oral protein delivery. *Proc. Natl. Acad. Sci. U.S.A.* **119**, e2207829119 (2022).
40. J. A. Nicolazzo, B. L. Reed, B. C. Finnin, Buccal penetration enhancers–How do they really work? *J. Control. Release* **105**, 1–15 (2005).
41. A. Kokate, X. Li, P. J. Williams, P. Singh, B. R. Jasti, In silico prediction of drug permeability across buccal mucosa. *Pharm. Res.* **26**, 1130–1139 (2009).
42. A. B. Nair, R. Kumria, S. Harsha, M. Attimarad, B. E. Al-Dhubiab, I. A. Alhaider, In vitro techniques to evaluate buccal films. *J. Control. Release* **166**, 10–21 (2013).

Acknowledgments: We thank K. Dubé (INRS) and M. Jutras (University of Montreal) for help with the in vivo experiments and analysis. Y. Ma and X. Ding are acknowledged for help in preparing the graphics. We thank N. Paunovic for proofreading the manuscript. **Funding:** This work was supported by the National Key Research and Development Program of China (no. 2022YFB3804700) to Z.L. and Guangdong Provincial Key Laboratory of Advanced Biomaterials (2022B1212010003) to Z.L. J.-C.L. acknowledges the funding from ETH Zurich Research Grants (no. 33 20-1). **Author contributions:** Z.L., D.K.C., and J.-C.L. conceptualized the study. Z.L., D.K.C., S.R., and N.Z. performed experiments and interpreted the results. Z.L. and J.-C.L. acquired funding and supervised the study. Z.L., D.K.C., and J.-C.L. wrote the manuscript. All authors critically read and approved the paper. **Competing interests:** Z.L., J.-C.L., and D.K.C. are coinventors on patent application EP21209752.1. Over the past 5 years, J.-C.L. had relationships with the following companies: Merck Sharp & Dohme, Inversago, MPeria, Xellia Pharmaceuticals, Hogan Lovells, TardiMed, Adocia, PK Med, Ascati Pharma, OM Pharma, Givaudan, Genfit, Inositec, and Versantis. The other authors declare that they have no competing interests. **Data and materials availability:** All data associated with this study are present in the paper or the Supplementary Materials. Raw and source data are available in Zenodo (doi:/10.5281/zenodo.6322663). Materials related to this paper may be provided by J.-C.L. through a material transfer agreement (MTA) with ETH Zurich.

Submitted 23 March 2022
Resubmitted 29 November 2022
Accepted 28 June 2023
Published 27 September 2023
10.1126/scitranslmed.abq1887

Science Translational Medicine

Boosting systemic absorption of peptides with a bioinspired buccal-stretching patch

Zhi Luo, David Klein Cerrejon, Simon Römer, Nicole Zoratto, and Jean-Christophe Leroux

Sci. Transl. Med. **15** (715), eabq1887. DOI: 10.1126/scitranslmed.abq1887

Science Translational Medicine (ISSN 1946-6242) is published by the American Association for the Advancement of Science. 1200 New York Avenue NW, Washington, DC 20005. The title *Science Translational Medicine* is a registered trademark of AAAS.